Complexing power of hydro-soluble degradation products from γ-irradiated polyvinylchloride: influence on Eu(OH)_3(s) solubility and Eu(III) speciation in neutral to alkaline environment

Pascal E. Reiller, Elodie Fromentin, Muriel Ferry, Adeline Dannoux-Papin, Hawa Badji, Michel Tabarant, Thomas Vercouter

Pascal E. Reiller*, Elodie Fromentin, Muriel Ferry, Adeline Dannoux-Papin, Hawa Badji, Michel Tabarant and Thomas Vercouter

Complexing power of hydro-soluble degradation products from γ-irradiated polyvinylchloride: influence on $Eu(OH)_3(s)$ solubility and Eu(III) speciation in neutral to alkaline environment

DOI 10.1515/ract-2016-2691
Received September 1, 2016; accepted January 27, 2017; published online March 22, 2017

Abstract: The complexing power of hydrosoluble degradation products (HDPs) from an alkaline hydrolysis of a 10 MGy γ-irradiated polyvinylchloride is studied. The complexation of Eu(III), as an analogue of lanthanide and actinide radionuclides at their +III oxidation state for oxygen containing functions, is evidenced both from the increasing of $Eu(OH)_3(s)$ dissolution, and from a complexometric titration by time-resolved luminescence spectroscopy. The dissolution of $Eu(OH)_3(s)$ in a simplified alkaline solution (0.3 M KOH/0.1 M NaOH) increases moderately, but significantly, with the HDPs concentration. The luminescence signal of the supernatant clearly indicates the presence of several complexed Eu(III) species. Performing a complexometric titration of Eu(III) from pH 6 by alkaline HDPs shows the formation of two different species with increasing HDPs' concentration and pH. Operational complexation constants – based on dissolved carbon concentration – are proposed. The analyses of the spectra and luminescence decays seem to confirm the presence of two different species.

Keywords: Europium, lanthanides, actinides, irradiated polymers, hydrosoluble degradation products, cementitious nuclear wastes.

***Corresponding author: Dr. Pascal E. Reiller,** PhD, Den – Service d'Etudes Analytiques et de Réactivité des Surfaces (SEARS), CEA, Université Paris-Saclay, F-91191 Gif-sur-Yvette CEDEX, France, E-mail: pascal.reiller@cea.fr
Elodie Fromentin and Muriel Ferry: Den – Service d'Etudes du Comportement des Radionucléides (SECR), CEA, Université Paris-Saclay, F-91191 Gif-sur-Yvette CEDEX, France
Adeline Dannoux-Papin: Den – Service des Procédés de Décontamination et d'Enrobage (SPDE), CEA, F-30207 Bagnols-sur-Cèze, France
Hawa Badji, Michel Tabarant and Thomas Vercouter: Den – Service d'Etudes Analytiques et de Réactivité des Surfaces (SEARS), CEA, Université Paris-Saclay, F-91191 Gif-sur-Yvette CEDEX, France

1 Introduction

Polymers are widely used in the nuclear industry: gloves or windows of glove-boxes, bottles, O-rings. During their use, these materials are in contact with radionuclides and suffer from radiolytic degradation. At the end of their service life, they are to be stored in intermediate-level long-lived waste (ILLW) packages in nuclear waste geological repositories, depending on national strategies. These packages are often cemented. Within the French concept, the ILLW packages would be stored in a deep underground clayey geological repository with cement backfill. During storage, the polymers will suffer from degradation by two phenomena: radio-oxidation and alkaline hydrolysis. Polymers are degraded by radio-oxidation, because of the presence of radionuclides (radiolytic degradation) and dioxygen (oxidation) into the waste packages. After repository closure, water will penetrate the repository and it will reach the packages' cores. This event is depending on the water permeability of the host rock. As the design of the repository and the waste packaging include an important amount of concrete, the water will become alkaline (around pH 13) when reaching the waste packages' cores [1].

Because of radio-oxidation and alkaline hydrolysis, organic hydro-soluble degradation products (HDPs) could be released in water. As an example, after γ irradiation of a plasticized poly(vinyl chloride) (PVC) under air up to 26 MGy, the identified HDPs obtained in alkaline water are largely additives, or degradation products from additives, such as phthalate ions, di-n-butyl phthalate, 2-ethylhexyl diphenyl phosphate and phenol [2]. In the same way, the HDPs from a radio-oxidized poly(ether urethane) were formed of alcohols, carboxylic acids and primary amines, as well as polyether oligomers with different end groups (aldehyde, alcohol or double bond) [3]. It turned out that the more radio-oxidized the polymer, the higher the oxidation rate of HDPs and the lower their molar mass. When the absorbed dose tends to be very

high, the expected HDPs for such a polymer should be low molar mass carboxylic acids, aldehydes and formic acid ester [4]. A very recent work succeeded in characterizing HDPs released from an industrial radio-oxidized poly(ester urethane) [5] hydrolysed in water. Short-organic acids such as acetic, formic, oxalic, malonic, glutaric, succinic, and adipic acids were identified and quantified. Other molecules were identified such as esters, alcohols, diols, ketones and polyester oligomers, confirming previous results [3].

From the very scarce literature on this topic, it is worth noting that HDPs nature and concentration depend on the studied polymer, its nature and additives. In addition, each study mentions that an appreciable amount of the pool of organic substances was not identified. Thus, there is a strong need to identify HDPs from the different polymers that could be present in the nuclear wastes.

Among these organic pools, the possibility to generate complexing entities is susceptible to lead to modification of radionuclides solubility in cementitious environment. A striking example is the formation of isosaccharinic acid during cellulose alkaline hydrolysis [6–8]. Another is the radiolytic degradation of ion exchange resins, producing short-chained organic molecules and an unknown pool of ligand [9–11]. Nevertheless, from the known complexation properties of short-chained organic molecules [12–15], it is most unlikely that an influence on the solubility of actinides may occur under cementitious conditions. The adsorption properties of these short-chained molecules are also relatively weak in cement [16]. Only carbohydrates, e.g. α-isosaccharinic acid, or polyaminocarboxylates, e.g. EDTA, could have an influence on actinides solubility in alkaline media [7, 15, 17, 18]. Phthalic acid, which is also known to form complexes in mildly acidic medium [19, 20], seems to form a mixed hydroxo complex with Eu(III), but the solid formed seems to be less soluble than $Eu(OH)_3$(s) [21].

Our aim is to investigate the global behaviour of an alkaline solution of HDPs obtained from a radio-oxidized PVC – under γ irradiation afterward cited as γ-PVC-HDP. As a preliminary step, it is chosen to analyse HDPs' interactions with europium(III), as a chemical analogue of trivalent lanthanides and actinides for oxygen containing functions [22]. PVC was irradiated under air at 10 MGy by γ-rays, and hydrolysed in alkaline water. First, the obtained solution was put in contact with $Eu(OH)_3$(s) under alkaline conditions and the solubility was measured by time-resolved luminescence spectroscopy (TRLS) and inductively coupled plasma-optic emission spectroscopy (ICP-OES). Second, a mildly acidic Eu(III) solution was titrated with the alkaline HDP solution to evidence by TRLS the potential Eu(III) complexation. The luminescence spectra and decays were analysed and discussed, and the global interaction constants were estimated. The implication of this complexing power on Eu(III) solubility in and out of a geological repository is then discussed.

2 Materials and methods

2.1 Chemicals

Additive-free PVC (grade K70) has been supplied in powder form by Plastunion (Bondy, France). $Eu(OH)_3$(s) was synthesized by forced hydrolysis, of $Eu(NO_3)_3 \cdot 6H_2O$ (Aldrich Co) in 10^{-2} M HNO_3. Solid $Eu(OH)_3$ was precipitated with KOH. The solid was dried at 60 °C for 2 days. The theoretical solubility of $Eu(OH)_3$(am) was calculated [23] – see thermodynamic data in Table S1 of the Supplementary Information (SI) –, and correction from non-ideality is made using the parameters from Kielland [24]. The limiting $Eu(CO_3)_3^{3-}$ complex [25] (Table S1 of the SI) is added to the model. As there is possible artefacts in the account of $Eu(OH)_4^-$ [23], only the first three hydroxo complexes were taken into account.

2.2 Preparation of γ-PVC-HDPs

Additive-free PVC was irradiated as received, under the form of films, at room temperature under air in open pillboxes using γ-rays (^{60}Co source) by IONISOS (Dagneux, France). A glass crystallizer was placed on the top of each pillbox to prevent dust deposition on the samples, while allowing air to flow inside the container. Dosimetry was performed using radiochromic (Red Perspex) dosimeters that were changed regularly. No electronic correction was made to account for the electronic density difference between water and additive-free PVC. The irradiation dose was 10 MGy and the mean dose rate was about 0.54 kGy/h. Uncertainties on given doses were less than 6%. The obtained solid γ-irradiated polymer (γ-PVC) were then used for the complexing power study of the alkaline HDPs.

The study of the complexing power of γ-PVC-HDPs is not straightforward in representative cement-pore waters. The composition of these pore waters is complex [26]. Even if simplified artificial pore waters were proposed [27], they

comprise calcium, which was shown to be a competitor for e.g. Th(IV) complexation by α-isosaccharinic acid [17]. Even if Vercammen et al. [7] did not evidence any effect of Ca^{2+} on the complexation of Eu(III) by α-isosaccharinic acid, it was decided to use an even simpler alkaline medium consisting of 0.3 M KOH and 0.1 M NaOH (pH ≈ 13.5) as a first step.

The alkaline extraction of γ-PVC-HDPs was done by contacting a weighed amount of approximately 1 g of solid γ-PVC in 10 g of 0.3 M KOH and 0.1 M NaOH previously degassed solution, under inert atmosphere (Ar) at 60 °C for 2 weeks in order to increase the extraction/hydrolysis kinetics. The obtained γ-PVC-HDPs solution was analysed in total organic carbon analysis (TOC-metre, Variotoc CUBE, Elementar) using weighed potassium hydrogenophthalate solutions as standards. After dilution by weighing, the carbon concentration of the γ-PVC-HDP solution was 21.1 ± 0.1 g_C/kg_w (211 $g_C/kg_{polymer}$, 1.76 mol_C/kg_w).

2.3 Dissolution of $Eu(OH)_3(s)$ in the presence of γ-PVC-HDPs

The pH value was measured using a combined glass electrode Inlab micro. The electrode was calibrated externally with four points, using commercial buffer solutions (pH 4.01, 7.01, and 10.00) plus a portlandite – $Ca(OH)_2(s)$ – suspension filtered just before use, which theoretical pH value is 12.7 at 22 °C. The linearity of the electrode response was checked and gave uncertainties better than 0.06 (1σ).

Different organic solutions were used for the solubility experiments. First, simulated solutions of varying total carbon concentration, consisting of four selected organic acids determined in HDPs, were used (Table 1). Phthalic acid, which is representative of plasticizers in different polymers, was used in additional solutions of varying total organic carbon.

From the known complexation constants of the lanthanides by these acids [12, 15, 19–21, 28–30], neither complexation of Eu(III) nor solubility enhancement of $Eu(OH)_3(s)$ at pH values relevant of cementitious environment are awaited. The account of other organic molecules recently evidenced [5] does not change the situation according to available thermodynamic data [31].

Second, weighed aliquots of 5 mg of $Eu(OH)_3(s)$ in 5 mg of the artificial alkaline water were placed in 10 mL centrifuge tubes. The synthetic solutions or γ-PVC-HDPs were added from weighed aliquots of the original solutions. After controlling the pH value, the tubes are closed under a flush of Ar. The solubility samples were placed under horizontal agitation for only one week in order to minimize $CO_2(g)$ contamination [32]. As the effect of ultracentrifugation on γ-PVC-HDPs is not known, the separation of phases was done by sedimentation. The formation of colloidal particles that could have stayed in the suspensions cannot be avoided, but is a common bias to every batch of these series.

2.4 Inductively coupled plasma-optic emission spectroscopy

For some samples the dissolved Eu concentrations in supernatants were quantified by ICP-OES (Perking Elmer Optima 2000 DV Spectrometer). Eu concentrations were determined at 412.970 nm and 381.967 nm using five or six points calibration curves (0–10,000 ppm); the uncertainties were better than 5%. Some samples were diluted before analysis to meet the concentration range of the calibration curve.

Table 1: Composition of the different synthetic solutions with total carbon concentration variation.

Sample	Concentration (mol/kg_w)						
	S1	**S2**	**S3**	**S4**	**S5**	**S6**	**S7**
Acetic	$1.53\ 10^{-4}$	$5.09\ 10^{-4}$	$1.53\ 10^{-3}$	$5.09\ 10^{-3}$	$1.53.10^{-2}$	$3.06\ 10^{-2}$	$7.64\ 10^{-2}$
Formic	$4.13\ 10^{-4}$	$1.38\ 10^{-3}$	$4.13\ 10^{-3}$	$1.38\ 10^{-2}$	$4.13.10^{-2}$	$8.26\ 10^{-2}$	$2.07\ 10^{-1}$
Oxalic	$3.55\ 10^{-4}$	$1.18\ 10^{-3}$	$3.55\ 10^{-3}$	$1.18\ 10^{-2}$	$3.55.10^{-2}$	$7.09\ 10^{-2}$	$1.77\ 10^{-1}$
Glutaric	$7.58\ 10^{-5}$	$2.53\ 10^{-4}$	$7.58\ 10^{-4}$	$2.53\ 10^{-3}$	$7.58.10^{-3}$	$1.52\ 10^{-2}$	$3.79\ 10^{-2}$
TOC mol_C/kg_w	$1.81\ 10^{-3}$	$6.02\ 10^{-3}$	$1.81\ 10^{-2}$	$6.02\ 10^{-2}$	$1.81\ 10^{-1}$	$3.83\ 10^{-1}$	$8.91\ 10^{-1}$
Sample	**P1**	**P2**	**P3**	**P4**	**P5**	**P6**	
Phthalic	$1.87\ 10^{-5}$	$5.14\ 10^{-5}$	$2.06\ 10^{-4}$	$5.64\ 10^{-4}$	$2.25\ 10^{-3}$	$1.25\ 10^{-1}$	
TOC mol_C/kg_w	$1.50\ 10^{-4}$	$4.12\ 10^{-4}$	$1.64\ 10^{-3}$	$4.52\ 10^{-3}$	$1.80\ 10^{-2}$	$9.99\ 10^{-1}$	

During the preconditioning for the typical ICP-OES analysis in 0.1 M HNO_3, sedimentation of the γ-PVC-HDPs were observed – see picture in Figure S1 of the SI. These supernatants were calcined and dissolved in 0.1 M HNO_3. Afterwards, it was decided to analyse the supernatants without acidification in ICP-OES by the standard addition method, and to double the analyses in TRLS in 3M K_2CO_3 [33], a medium which maintains the alkalinity of the solution and enhances the luminescence of Eu(III) through the formation of $Eu(CO_3)_3^{3-}$ complex.

2.5 Time-resolved luminescence spectroscopy

The experimental set-up, luminescence spectra acquisitions, luminescence decay times fitting, and fitting uncertainties estimations have been described elsewhere [34–36]. A 300 lines/mm grating (Princeton, Evry, France) was used. The luminescence signal was collected during a time gate width (*W*) of 300 µs, at an initial delay time (*D*) of 10 µs after the excitation laser pulse. To increase the signal-to-noise ratio, 300–1000 accumulations were performed for each spectrum. All measurements were carried on at room temperature (20 °C). The excitation wavelength was set in the $^5L_6 \leftarrow {}^7F_0$ transition of Eu(III) (λ_{exc} = 393.7 nm) [37]. For each obtained spectrum a background correction was performed.

2.5.1 Eu(III) concentration analysis in the supernatants

For the Eu(III) concentration analyses, a weighed 1 mL aliquot was sampled into a 1 cm quartz cuvette, and the necessary amount of solid K_2CO_3 was weighed and added to the aliquot to provide the 3 M medium. The concentration of Eu was determined using the standard addition method. The standard was obtained from the dissolution of 99.99% Eu_2O_3 (Johnson Matthey, Roissy, France) in 3 M K_2CO_3 – all amounts were weighed. The area under the $^5D_0 \rightarrow {}^7F_2$ transition (trapezoid method) was plotted vs. the added (weighed amounts of typically 10–100 µL) concentrations of standard.

2.5.2 Eu(III) speciation in the presence of γ-PVC-HDP

Eu(III) spectra with increasing concentration of γ-PVC-HDP were obtained from an initial 10^{-6} M Eu solution at pH 6 in 0.1 M NaCl. This solution was prepared from a 10^{-3} M stock solution obtained after the dissolution of 99.99% Eu_2O_3 (Johnson Matthey, Roissy, France) in 3.5 10^{-3} M HCl. Weighed amounts of γ-PVC-HDP were added to a 1.5 mL aliquot of the 10^{-6} M Eu solution. Some solutions were kept for at least 3 weeks and checked regularly for luminescence signal modification due to eventual precipitation of either $Eu(OH)_3$(am) or $EuOHCO_3$(cr).

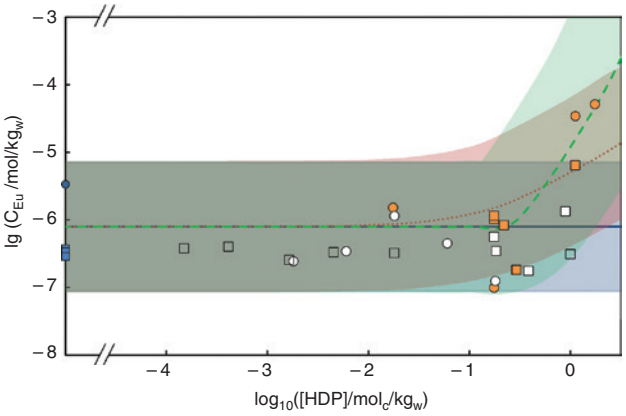

Figure 1: Dissolution of $Eu(OH)_3$(s) in artificial alkaline solution (KOH 0.3/NaOH 0.1 M) at varying carbon concentration of synthetic solutions and γ-PVC-HDPs, analysed in ICP-OES (circles), and in TRLS (squares): blue symbols are the Eu dissolution with no organics added, orange symbols are for γ-PVC-HDPs, white symbols are for the short-chained mix of acids, empty symbols are for phthalic acid; blue line is the theoretical solubility of $Eu(OH)_3$(am) based on thermodynamic constants [23, 25] and blue zone is the calculated uncertainty on Eu solubility, red dotted line is the operational solubility curves considering the formation of $Eu(OH)_3$(HDP) and green dashed line is the operational solubility curves considering the formation of $Eu(OH)_2(HDP)_3$, with the red and green zones being the same uncertainty as the blue zone.

3 Results and discussion

3.1 Solubility of $Eu(OH)_3$(s)

Results obtained by ICP-OES and TRLS are shown in Figure 1. As awaited from the already known complexation constants from the "simple" organic molecules – *vide ante* –, no significant increase of the $Eu(OH)_3$(s) solubility is evidenced in 0.3 M KOH/0.1 M NaOH neither for the organic acids nor for phthalic acid. Nevertheless, a significant increase by one and a half order of magnitude of the Eu(III) concentration in the supernatant is observed for γ-PVC-HDP concentration higher than 1 mol_C/kg_w, either from ICP-OES or TRLS results.

The determination of formation constants seems awkward considering our lack of knowledge of the types

of chemical functions that are engaged in complexation reactions and their amounts. Titration experiments would be desirable, but were not performed up to now due to the very low amount of γ-PVC-HDPs' solution available and the amount of products that is usually necessary for e.g. natural organic products [38–40]. It is nevertheless tempting to calculate an operational complexation constant, K_{op}, relative to the total carbon concentration in solution – omitting the charges of the complex because of our lack of knowledge on γ-PVC-HDP functionality.

$$Eu^{3+} + nH_2O + m\,HDP \rightleftarrows Eu(OH)_n(HDP)_m + nH^+$$
$$K_{op} = \frac{[Eu(OH)_n(HDP)_m]\,[H^+]^n}{[Eu^{3+}]\,[HDP]^m} \quad (1)$$

Unfortunately, the increase of the solubility is quite limited. Several hypotheses can be proposed combining different values of *n* and *m*. First, as the major Eu(III) species at this pH value is $Eu(OH)_3$(aq), one can propose the formation of $Eu(OH)_3$(HDP). The dotted line on Figure 1 is obtained from the above operational equilibrium considering that $Eu(OH)_3$(aq) is major in solution under our conditions yielding $Eu(OH)_3$(HDP), and that 1 mole of carbon from HDP is implied. The increase in $Eu(OH)_3$(s) dissolution is poorly represented with an operational $\log_{10}K_{op} = -23.7$ ($r^2 = 0.429$).

One can also consider that a lower hydrolysed species is forming a complex. As the increase in solubility seems to follow a slope of +3, $Eu(OH)_2(HDP)_3$, a combination of two moles of H_2O for three moles of carbon in HDPs (dotted line), would better represent the evolution in Figure 1, with an operational $\log_{10}K_{op} = -9.9$ ($r^2 = 0.743$). From the low amount of available data, due to the low amount of available sample and the small increase in $Eu(OH)_3$(s) solubility, it is difficult to firmly discriminate one hypothesis from the other.

3.2 Luminescence of Eu(III) in the presence of γ-PVC-HDPs

The Eu(III) luminescence spectra of the supernatant of solubility experiments of $Eu(OH)_3$(s), and after 1 or 2 days in contact with γ-PVC-HDPs – before adding K_2CO_3 – are shown in Figure S2 of the SI. In addition to a remaining luminescence due to the γ-PVC-HDPs, the luminescence of solubilized Eu(III) can be clearly observed. The $^5D_0 \rightarrow {}^7F_2$ transition dominating the spectrum at λ_{max} approximately 615 nm indicates the formation of a complex.

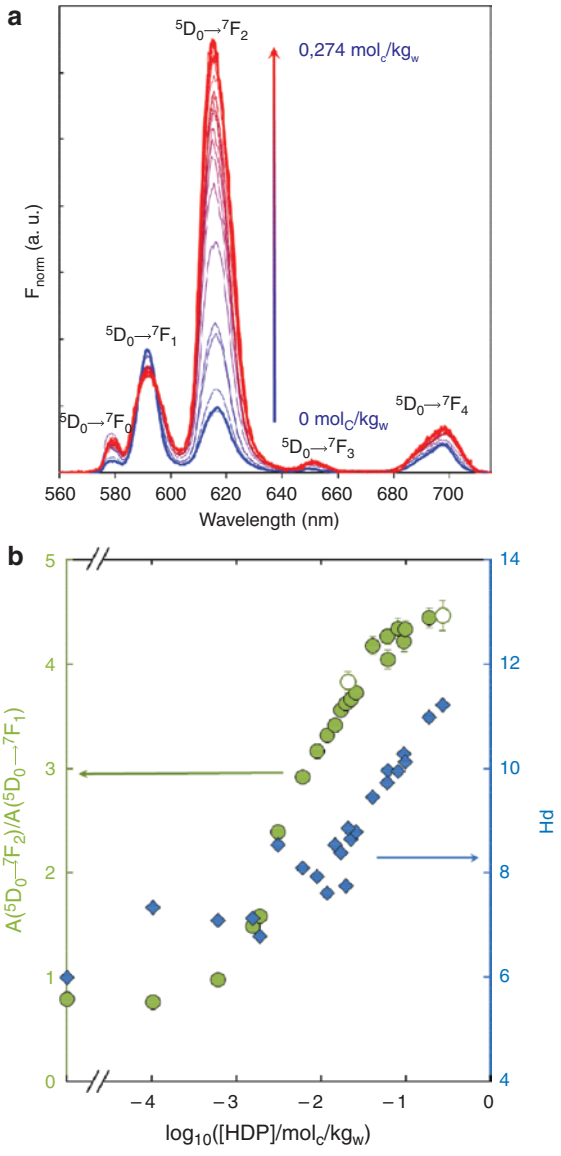

Figure 2: Evolutions with the γ-PVC-HDPs concentration (mol$_c$/kg$_w$) of (a) the luminescence spectra of Eu(III) normalized to the area of the $^5D_0 \rightarrow {}^7F_1$ transition – from 0 blue thick line to 0.274 mol$_c$/kg$_w$ red thick line –, and (b) the $^7F_2/{}^7F_1$ asymmetry ratio (circles) and solution pH (diamonds); [Eu] = 1 µM, *D* = 10 µs, *W* = 300 µs, λ_{exc} = 393.7 nm, *I* = 0.1 M NaCl; empty circles represent experiments for which decay time measurements are presented in Figure 4. Error bars represent 2σ of the $^7F_2/{}^7F_1$ asymmetry ratio using the trapezoid method.

3.2.1 Complexation of Eu(III) by γ-PVC-HDPs

The evolution of the luminescence of Eu(III) from pH 6 (0.1 M NaCl), by adding γ-PVC-HDPs is shown normalized to the area of the $^5D_0 \rightarrow {}^7F_1$ transition in Figure 2a, and normalized to the 560–715 nm span in Figure S3 of the SI. The presence of the $^5D_0 \rightarrow {}^7F_0$ transition indicates the presence

of at least one species other than Eu^{3+}, although it may be a minor species. The variation of the intensity of the $^5D_0 \rightarrow {}^7F_0$ transition in Figure S4 of the SI, issued from Figure S3 of the SI, suggests that several mechanisms are taking place. First, an increase of the $^5D_0 \rightarrow {}^7F_0$ relative intensity up to 3 10^{-3} mol_C/kg_W suggests a loss of centro-symmetry of the complex. Second, a further decrease of the $^5D_0 \rightarrow {}^7F_0$ relative intensity to values lower than the original one at pH 6 and no carbon added suggests that the final complex is more centro-symmetric.

The complexation of Eu(III) by the γ-PVC-HDPs is also evidenced by the typical change in the area ratio $^5D_0 \rightarrow {}^7F_2/{}^5D_0 \rightarrow {}^7F_1$ transitions (Figure 2b), commonly defined as the $^7F_2/{}^7F_1$ asymmetry ratio. The initial $^7F_2/{}^7F_1$ ratio of 0.8 – instead of ca. 0.3 for Eu^{3+} – further indicates that the initial Eu(III) signal cannot be only attributed to Eu^{3+} [30, 34, 36]. The increasing asymmetry ratio and the variation of the $^5D_0 \rightarrow {}^7F_0$ transition with the γ-PVC-HDPs carbon concentration indicate changes in the symmetry of the complex(es). The full width at half height of the $^5D_0 \rightarrow {}^7F_1$ transition is gradually increasing, and the $^5D_0 \rightarrow {}^7F_2$ is slightly blue-shifted. The $^5D_0 \rightarrow {}^7F_3$ and $^5D_0 \rightarrow {}^7F_4$ transitions relative intensities are slightly decreasing and red-shifted (Figure S3 of the SI).

The obtained spectra are clearly different from either Eu(III) hydroxo complexes but also from $Eu(CO_3)_n^{3-2n}$ complexes [25, 41, 42]. The plot of the asymmetry ratio (Figure 2b) is typically showing the formation of at least one complex with increasing carbon concentration and pH. Speciation diagrams under different conditions are calculated in Figure S5 of the SI [23, 25]. Under our conditions, either $Eu(OH)_3(am)$ – if no $CO_2(g)$ is present in Figure S5a of the SI – or $EuOHCO_3(cr)$ – in an open system in Figure S5c of the SI – should precipitate under mildly alkaline conditions. In a closed system – as in spectroscopic cuvettes, two volumes of air over one volume of water –, $EuOHCO_3(cr)$ should precipitate between pH 7 and 10.2, and then $Eu(OH)_3(am)$ should be in equilibrium with $Eu(OH)_3(aq)$ at higher pH values (Figure S5e of the SI). We did not observe any precipitation nor any change in the Eu(III) luminescence signal over the course of the experiments – the sample with γ-PVC-HDPs of the highest carbon concentration and at pH 11.2 was kept, and the TRLS signal and spectrum checked, for several weeks. The presence of a complex is in agreement with the enhanced $Eu(OH)_3(s)$ solubility observed previously at higher pH.

As stressed earlier, the determination of the formation constants can only be global without the knowledge of γ-PVC-HDPs functionality. Following the same reasoning, which has been used in solubility interpretation, and considering the simple equilibrium between non-complexed europium (Eu_{nc}) and γ-PVC-HDPs, one can write the following operational equilibrium with associated operational constant K_{op}.

$$Eu_{nc} + m\text{HDP} \rightleftarrows Eu(\text{HDP})_m$$
$$K_{op,Eu} = \frac{[Eu(\text{HDP})_m]}{[Eu]_{nc}\,[\text{HDP}]^m} \quad (2)$$

The plot of $\log_{10}([Eu(\text{HDP})_m]/[Eu]_{nc})$ vs. $\log_{10}[\text{HDP}]$ in Figure 3a gives a slope close to unity (Table 2) and $\log_{10}K_{op,Eu} = 3.23 \pm 0.09$ (1σ) at the intercept on the basis of the carbon concentration of γ-PVC-HDPs.

This operational constant can also be plotted against the free ion Eu^{3+} concentration considering the hydrolysis constants of Eu(III) [23, 25].

$$[Eu]_{nc} = [Eu^{3+}]\left(1 + \sum \frac{{}^*\beta_n}{[H^+]^n}\right) = \alpha(Eu^{3+})\,[Eu^{3+}] \quad (3)$$

The plot of $\log_{10}([Eu(\text{HDP})_m/[Eu^{3+}])$ vs. $\log_{10}[\text{HDP}]$ in Figure 3b gives two straight lines: the first is showing a slope close to 2 (Table 2) with $\log_{10}K_{op,1,Eu^{3+}} = 5.5 \pm 1.1$ (1σ), and the second slope is close to 8 with $\log_{10}K_{op,2,Eu^{3+}} = 16.1 \pm 0.8$ (1σ). It is worth to notice that the uncertainty on the first straight line parameters is rather high, and that the high carbon concentration part is giving a high number of carbon implied in complexation.

The slope analyses can also be done considering the other hydroxo complexes. The calculation of the Ringböm's coefficients for the different hydroxo complexes – $\alpha(EuOH^{2+})$, $\alpha(Eu(OH)_2^+)$, and $\alpha(Eu(OH)_3(aq))$ – are recalled in the SI and the equivalent plots of equation (3) for each hydroxo complex is shown in Figure S6 of the SI. The slopes, $\log_{10}K_{op}$, and determination coefficient (r^2) are reported in Table 2. First, it can be noted that all the plots of $\log_{10}([Eu(\text{HDP})_n/[Eu(OH)_n^{(3-n)+}])$ vs. $\log_{10}[\text{HDP}]$ in Figure S6 of the SI are showing a change in slopes at $\log_{10}[\text{HDP}]$ approximately –1.7, i.e. 0.02 mol_C/kg_w, for every situation. This indicates that two species are likely to occur during the complexometric titration. Accounting for $\alpha(Eu(OH)_3(aq))$ is leading to non-sense negative slope in the first part of the isotherm and to a slope of 0 in the second part, which suggests that this species is not likely in interaction with HDPs. The interaction with $Eu(OH)_2^+$ is also unlikely in the first part of the isotherm as a slope of 0 is obtained; a slope of 2.6 is obtained in the second part of the isotherm. The use of $\alpha(Eu(OH)^{2+})$ (Figure 3c) is showing two slopes, the first one being close to unity, and the second close to 5, with r^2 being slightly higher than for $\alpha(Eu^{3+})$.

It is also possible to express these constants related to Eu^{3+}, using thermodynamic hydrolysis constants corrected

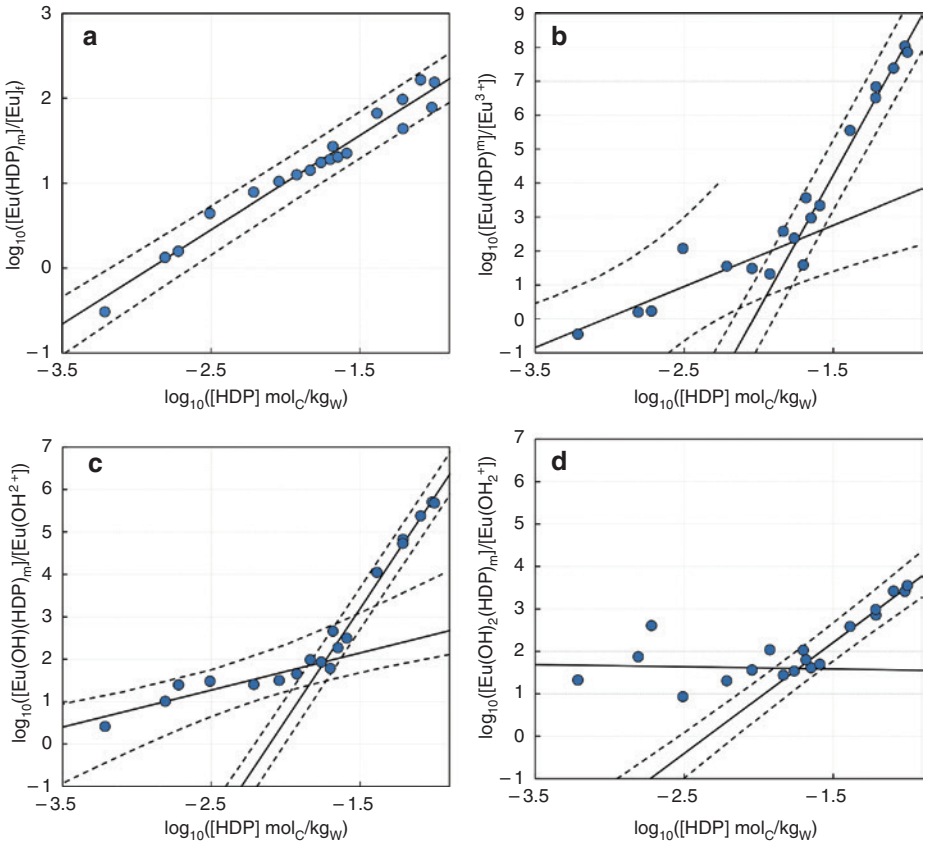

Figure 3: Determination of the Eu(III)-HDP complexes' stoichiometries – on mol_C/kg_w basis – and apparent formation constants K_{op} from TRLS results from Figure 2 considering (a) total non-complexed europium, (b) Eu^{3+} free, (c) $EuOH^{2+}$, and (d) $Eu(OH)_2^+$ in solution using hydrolysis constants [23]; $[Eu(III)]_{total} = 10^{-6}$ mol/kg_w, $I = 0.1$ M NaCl.

Table 2: Possible slope analyses of Figure 3 and Figure S6 of the SI. Charges are omitted because of the lack of knowledge on the functionality of γ-PVC-HDPs.

Equilibrium	Slope	r^2	$\log_{10} K_{op}$
$Eu + HDP \leftrightarrows EuHDP$	1.11 ± 0.05	0.9680	3.23 ± 0.09
$Eu^{3+} + 2\ HDP \leftrightarrows Eu(HDP)_2$	1.8 ± 0.5	0.7108	5.5 ± 1.1
$Eu^{3+} + 8\ HDP \leftrightarrows Eu(HDP)_8$	7.9 ± 0.5	0.9611	16.1 ± 0.8
$Eu(OH)^{2+} + HDP \leftrightarrows Eu(OH)HDP$	0.9 ± 0.2	0.8203	3.5 ± 0.4
$Eu^{3+} + H_2O + HDP \leftrightarrows Eu(OH)HDP + H^+$			−4.3 ± 0.4
$Eu(OH)^{2+} + 5\ HDP \leftrightarrows Eu(OH)(HDP)_5$	5.3 ± 0.3	0.9799	11.1 ± 0.4
$Eu^{3+} + H_2O + 5HDP \leftrightarrows Eu(OH)(HDP)_5 + H^+$			3.3 ± 0.4
$Eu(OH)_2^+ + 3\ HDP \leftrightarrows Eu(OH)_2(HDP)_3$	2.6 ± 0.2	0.9536	6.1 ± 0.3
$Eu^{3+} + 2H_2O + 2HDP \leftrightarrows Eu(OH)_2(HDP)_3 + 2H^+$			−9.6 + 0.3

to 0.1 M NaCl [23, 24]. Interestingly, the value obtained relative to the complexation of $Eu(OH)_2^+$ in the second part of the isotherm is in very good agreement with the possible constant obtained in dissolution experiment using the formation of $Eu(OH)_2(HDP)_3$ on carbon concentration basis. One must here remind that these stoichiometries are based on the quantities of carbon involved in the complexation reaction. They do not give directly the stoichiometry of the functions implied in the complexation. It is also worthy to notice that the pH dependence should also include the acid base properties of HDPs. The mixed hydroxo complexes of Eu(III) with natural organic matter was proven not to be necessary in the modelling [36]. Further works are needed to confirm these observations, and obtain complexation constants based on the functionality quantification. Hence, for further use of speciation calculation we would use the equilibria implying Eu(OH)(HDP) and $Eu(OH)_2(HDP)_3$.

3.2.2 Decay time evolution

To help interpreting the slope analyses, the decay time evolutions of two particular points of Figure 2 – pH 8.85, $\log_{10}[HDP] = -1.68$; and pH 11.21, $\log_{10}[HDP] = -0.56$ – are presented in Figure 4 – time-resolved spectra in Figure S8 of the SI. The first striking feature is the presence of a bi-exponential decay for the two cases – correlation matrices in Table S2 of the SI. The values of τ_1 are faster than Eu^{3+} (110 μs) [43]. If this feature is commonly observed for natural organic complexes of Eu(III) [34–36, 44], this is to our knowledge the first observation for anthropogenic organic samples. Faster than Eu^{3+} mono-exponential decays were also evidenced for hydroxybenzoic acids complexes [30, 45, 46]. The τ_2 values are slower than that of natural organic complexes of Eu(III) [34–36, 44].

Applying the relationship from Kimura and Choppin [47] to the τ_2 values, approximately 3.2 (Figure 2a) and 2.3 (Figure 2b) water molecules (±0.5) remain in the first hydration sphere of the Eu-HDP complex(es). Then, at the end of the complexation reaction – empty points in Figure 2b – only two water molecules are still in the first hydration sphere of Eu(III). Knowing that 8–9 water molecules are involved in the first hydration of Eu^{3+} [48], 6–7 positions should be occupied. As we only have access to the amount of carbon implied in the complexation process, it seems awkward to propose a denticity for Eu-HDP complexes. Moreover, the application of the relationship from Kimura and Choppin [47] has not been firmly established in the case of hydroxo complexes of Eu(III) [41]. Nevertheless, from the concordant data on $Eu(OH)_2(HDP)_3$ one can await that the complexes have at least a certain degree of multi-denticity.

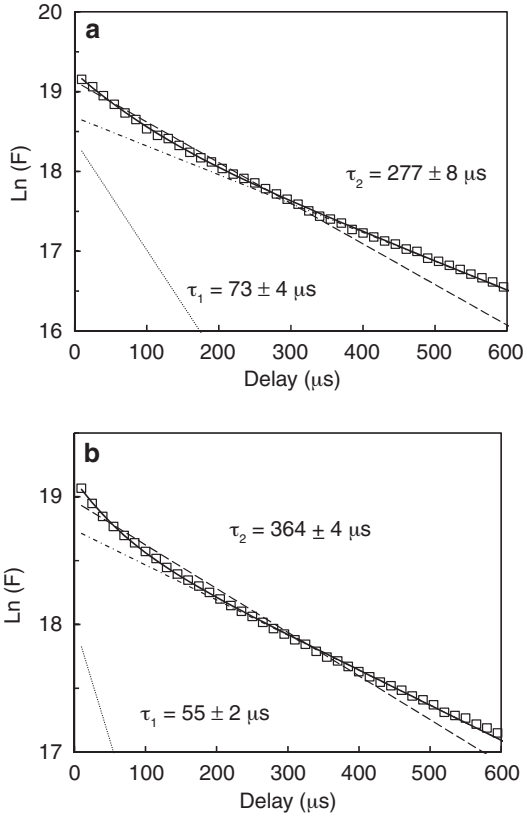

Figure 4: Luminescence decays of Eu(III) at (a) 0.021 mol_C/kg_w (pH 8.85, $\log_{10}([HDP]/mol_C/kg_w) = -1.68$) and (b) 0.274 mol_C/kg_w (pH 11.21, $\log_{10}([HDP]/mol_C/kg_w) = -0.56$) of γ-PVC-HDPs. Calculated on the area of the $^5D_0 \rightarrow {}^7F_2$ transition, $W = 300$ μs, $\lambda_{exc} = 393.7$ nm; plain line is the bi-exponential decay composed of a fast (dotted) and a slow (dash-dot) component, and dashed line is the mono-exponential decay. Uncertainties on decay times are fitting uncertainties.

4 Implication on Eu(III) solubility and speciation in the pH/C(γ-PVC-HDP) studied domain

The solubility surfaces of total 0.01 M $Eu(OH)_3(am)$ as a function of pH and γ-PVC-HDP concentration can be drawn (Figure 5a), using the formation constants for Eu(OH)(HDP) and $Eu(OH)_2(HDP)_3$ given in Table 2. First, it appears clearly that important amount of γ-PVC-HDPs are needed as important carbon concentration are necessary to obtain a significant solubilisation of $Eu(OH)_3(s)$. The solubility of $Eu(OH)_3(am)$ is seen noticeably enhanced at the lowest pH and highest γ-PVC-HDP concentration values, but seems limited to less than two orders of magnitude for ca. 1 mol_C/kg_w – which was the amount of carbon concentration used here. Nevertheless, the calculated solubility is decreasing with pH – due to the dependence on $[H^+]^n$ –, which induces that the affinity of γ-PVC-HDP for Eu(III) increases when pH is decreasing. It means that the influence of γ-PVC-HDP on lanthanides(III) or actinides(III) extends down to mildly alkaline pH media, such as argillaceous host rock conditions [49–51].

In addition, the solubility surfaces of $EuOHCO_3(cr)$ with and without the γ-PVC-HDP at $PCO_2(g) = 10^{-3.5}$ atm – limited in the pH span 6–9.5 – is drawn in Figure 5b. Here again the solubility of the phase is slightly enhanced at higher pH and more important at lower pH, as the solubility of $EuOHCO_3(cr)$ is increased by four orders of magnitude ca. pH 8.5 and 1 mol_C/kg_w. The influence should be lower at $PCO_2(g) = 10^{-2}$ atm – as for typical equivalent partial pressure for argillaceous rocks [50, 51], see Figure S7 of the SI –, as the increase is approximately two orders of magnitude at pH 8.5.

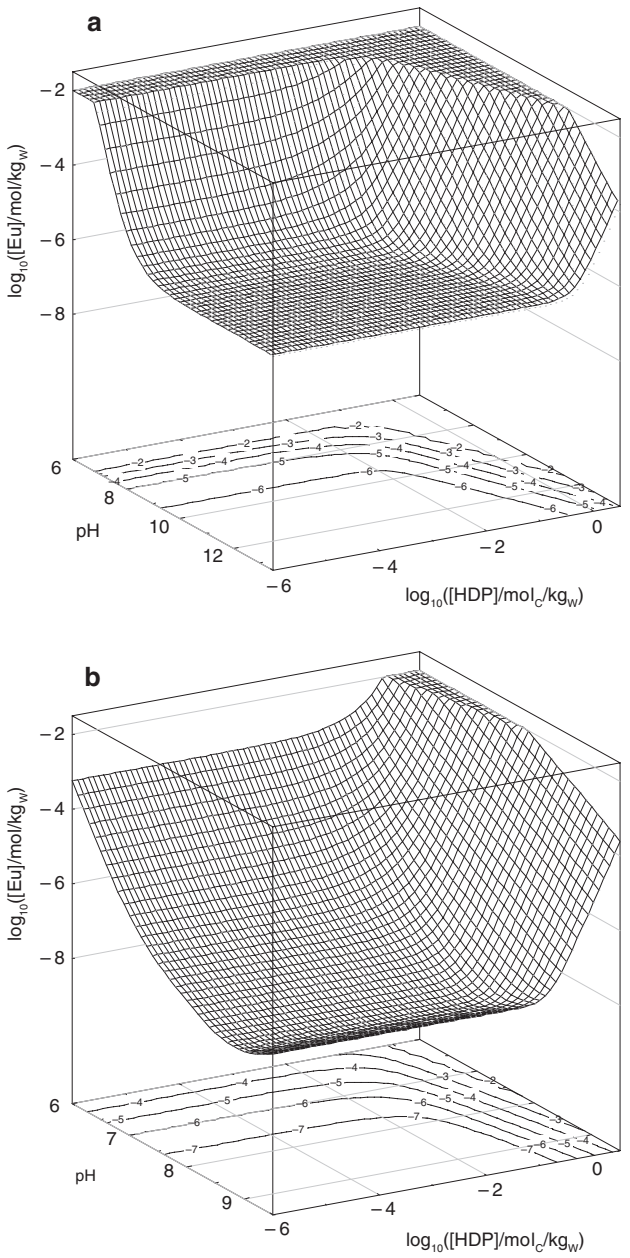

Figure 5: Evolution of the solubility surfaces of $[Eu]_{tot} = 10^{-2}$ mol/kg_w as a function of pH and concentration of γ-PVC-HDP, on total carbon basis, using thermodynamic constants [23, 25] and formation constants for Eu(OH)(HDP) and $Eu(OH)_2(HDP)_3$ in Table 2 of (a) $Eu(OH)_3$(am) at $PCO_2(g) = 10^{-12}$ atm, and (b) $EuOHCO_3$(cr) at $PCO_2(g) = 10^{-3.5}$ atm.

5 Conclusions

From these experiments, it seems clear that the complexation of Eu(III) by γ-PVC-HDPs can occur under cementitious conditions, but also under more neutral conditions as in argillaceous host rocks. The slight but significant increase of $Eu(OH)_3$(s) dissolution, the evolution of the TRLS signal in the supernatant from dissolution experiments, the TRLS titration of Eu(III) by γ-PVC-HDPs, and the decay times analyses are all converging to this conclusion. It seems that several complexes are occurring, but the exact stoichiometry is still difficult to assess. From our experiments, as awaited from the thermodynamic data available, the synthetic solutions do not seem to increase the dissolution of $Eu(OH)_3$(s) in alkaline medium. The amount of HDPs, on carbon concentration basis, needed to have an appreciable effect on the solubility in high alkaline media, and the operational formation constants (K_{op}), allow providing a global evaluation of the γ-PVC-HDPs impact, knowing their inventory in the wastes.

Further works are needed, particularly in the light of more recent identification of molecules in γ-PVC-HDPs [5] to ascertain the composition of these γ-PVC-HDPs, their functionality – particularly the organic moieties that are responsible of these complexation reactions – and to determine the variability of the complexing moieties as a function of the polymer and the γ-ray dose. The interactions of these organic moieties with cementitious phases [32, 52] should also be of interest to appreciate their retardation in cements before reaching the host rock.

Acknowledgements: Camille Auriault and Daniel Léonço are acknowledged for their participation in the experimental dissolution and TRLS work. Soumaya Boughattas is acknowledged for the synthesis of $Eu(OH)_3$(s). Dr. Nathalie Macé is acknowledged for her support during the TOC analyses. This work was financed by AREVA, Andra, and CEA within the framework of the COSTO project from CEA. Dr. Christine Lamouroux-Lucas is acknowledged for her strong support.

References

1. Berner, U. R.: Evolution of pore water chemistry during degradation of cement in a radioactive waste repository environment. Waste Manage. **12**, 201 (1992).
2. Colombani, J., Herbette, G., Rossi, C., Joussot-Dubien, C., Labed, V., Gilardi, T.: Leaching of plasticized PVC: effect of irradiation. J. Appl. Polym. Sci. **112**, 1372 (2009).
3. Dannoux, A.: Extrapolation dans le temps des cinétiques de production des produits de dégradation radiolytique : application à un polyuréthane (2007), PhD Thesis, Université Paris XI, Orsay, France, p. 270.
4. Dannoux, A., Esnouf, S., Amekraz, B., Dauvois, V., Moulin, C.: Degradation mechanism of poly(ether-urethane) Estane® induced by high-energy radiation. II. Oxidation effects. J. Polym. Sci., Part B: Polym. Phys. **46**, 861 (2008).

5. Fromentin, E., Pielawski, M., Lebeau, D., Esnouf, S., Cochin, F., Legand, S., Ferry, M.: Leaching of radio-oxidized poly(ester urethane): water-soluble molecules characterization. Polym. Degrad. Stab. **128**, 172 (2016).
6. Bourbon, X., Toulhoat, P.: Influence of organic degradation products on the solubilisation of radionuclides in intermediate and low level radioactive wastes. Radiochim. Acta **74**, 315 (1996).
7. Vercammen, K., Glaus, M. A., Van Loon, L. R.: Complexation of Th(IV) and Eu(III) by α-isosaccharinic acid under alkaline conditions. Radiochim. Acta **89**, 393 (2001).
8. Glaus, M. A., Van Loon, L. R.: Degradation of cellulose under alkaline conditions: new insights from a 12 years degradation study. Environ. Sci. Technol. **42**, 2906 (2008).
9. Van Loon, L. R., Hummel, W.: Radiolytic and chemical degradation of strong acidic ion-exchange resins: study of the ligands formed. Nucl. Technol. **128**, 359 (1999).
10. Van Loon, L. R., Hummel, W.: The degradation of strong basic anion exchange resins and mixed-bed ion-exchange resins: effect of degradation products on radionuclide speciation. Nucl. Technol. **128**, 388 (1999).
11. Hummel, W., Van Loon, L. R.: The effect of degradation products of strong acidic cation exchange resins on radionuclide speciation: a case study with Ni^{2+}. Nucl. Technol. **128**, 372 (1999).
12. Choppin, G. R., Dadgar, A., Rizkalla, E. N.: Thermodynamics of complexation of lanthanides by dicarboxylate ligands. Inorg. Chem. **25**, 3581 (1986).
13. Lajunen, L. H. J., Portanova, R., Piispanen, J., Tolazzi, M.: Critical evaluation of stability constants for *alpha*-hydroxycarboxylic acid complexes with protons and metal ions and the accompanying enthalpy changes – Part I: aromatic *ortho*-hydroxycarboxylic acids. Pure Appl. Chem. **69**, 329 (1997).
14. Portanova, R., Lajunen, L. H. J., Tolazzi, M., Piispanen, J.: Critical evaluation of stability constants for *alpha*-hydroxycarboxylic acid complexes with protons and metal ions and the accompanying enthalpy changes – Part II: aliphatic 2-hydroxycarboxylic acids. Pure Appl. Chem. **75**, 495 (2003).
15. Hummel, W., Anderegg, G., Rao, L. F., Puigdomènech, I., Tochiyama, O.: Chemical Thermodynamics 9. Chemical Thermodynamics of Compounds and Complexes of U, Np, Pu, Am, Tc, Se, Ni and Zr with Selected Organic Ligands (2005), North Holland Elsevier Science Publishers B. V., Amsterdam, The Netherlands, p. 1088.
16. Wieland, E., Jakob, A., Tits, J., Lothenbach, B., Kunz, D.: Sorption and diffusion studies with low molecular weight organic compounds in cementitious systems. Appl. Geochem. **67**, 101 (2016).
17. Vercammen, K., Glaus, M. A., Van Loon, L. R.: Evidence for the existence of complexes between Th(IV) and α-isosaccharinic acid under alkaline conditions. Radiochim. Acta **84**, 221 (1999).
18. Vercammen, K., Glaus, M. A., Van Loon, L. R.: Complexation of calcium by α-isosaccharinic acid under alkaline conditions. Acta Chem. Scand. **53**, 241 (1999).
19. Wang, Z. M., van de Burgt, L. J., Choppin, G. R.: Spectroscopic study of lanthanide(III) complexes with carboxylic acids. Inorg. Chim. Acta **293**, 167 (1999).
20. Thakur, P., Conca, J. L., Choppin, G. R.: Complexation studies of Cm(III), Am(III), and Eu(III) with linear and cyclic carboxylates and polyaminocarboxylates. J. Coord. Chem. **64**, 3215 (2011).
21. Park, K. K., Jung, E. C., Cho, H. R., Kim, W. H.: Ternary complex formation of Eu(III) with o-phthalate in aqueous solutions. Spectrochim. Acta, Part A **73**, 615 (2009).
22. Pearson, R. G.: Hard and soft acids and bases. J. Am. Chem. Soc. **85**, 3533 (1963).
23. Hummel, W., Berner, U., Curti, E., Pearson, F. J., Thoenen, T.: Nagra/PSI chemical thermodynamic data base 01/01 (2002), NAGRA, Report NTB 02-06, Parkland, FL, USA. p. 564.
24. Kielland, J.: Individual activity coefficients of ions in aqueous solutions. J. Am. Chem. Soc. **59**, 1675 (1937).
25. Vercouter, T., Vitorge, P., Trigoulet, N., Giffaut, E., Moulin, C.: $Eu(CO_3)_3^{3-}$ and the limiting carbonate complexes of other M^{3+} f-elements in aqueous solutions: a solubility and TRLFS study. New J. Chem. **29**, 544 (2005).
26. Berner, U. R.: Modeling the incongruent dissolution of hydrated cement minerals. Radiochim. Acta **44–45**, 387 (1988).
27. Berner, U. R.: A Thermodynamic Description of the Evolution of Pore Water Chemistry and Uranium Speciation during the Degradation of Cement (1990), Nagra, Report PSI Bericht 62, Paul Scherrer Institut, Villigen, Switzerland, and TR-90-12, Wettingen, Switzerland.
28. Macero, D. J., Anderson, L. B., Malachesky, P.: Voltammetric studies of Eu(III) in formate buffer – Formal potential of Eu(III)-Eu(II) system. J. Electroanal. Chem. **10**, 76 (1959).
29. Pascual, E. G., Choppin, G. R.: The thermodynamics of complexation of lanthanides by o-phthalic acid. Lanthanide Actinide Res. **1**, 57 (1985).
30. Moreau, P., Colette-Maatouk, S., Vitorge, P., Gareil, P., Reiller, P. E.: Complexation of europium(III) by hydroxybenzoic acids: a time-resolved luminescence spectroscopy study. Inorg. Chim. Acta **432**, 81 (2015).
31. Wang, Z. M., van de Burgt, L. J., Choppin, G. R.: Spectroscopic study of lanthanide(III) complexes with aliphatic dicarboxylic acids. Inorg. Chim. Acta **310**, 248 (2000).
32. Pointeau, I., Hainos, D., Coreau, N., Reiller, P.: Effect of organics on selenite uptake by cementitious materials. Waste Manage. **26**, 733 (2006).
33. Berthoud, T., Decambox, P., Kirsch, B., Mauchien, P., Moulin, C.: Direct determination of traces of lanthanide ions in aqueous-solutions by laser-induced time-resolved spectrofluorimetry. Anal. Chim. Acta **220**, 235 (1989).
34. Brevet, J., Claret, F., Reiller, P. E.: Spectral and temporal luminescent properties of Eu(III) in humic substance solutions from different origins. Spectrochim. Acta, Part A **74**, 446 (2009).
35. Reiller, P. E., Brevet, J.: Bi-exponential decay of Eu(III) complexed by Suwannee River humic substances: spectroscopic evidence of two different excited species. Spectrochim. Acta, Part A **75**, 629 (2010).
36. Kouhail, Y. Z., Benedetti, M. F., Reiller, P. E.: Eu(III)-fulvic acid complexation: evidence of fulvic acid concentration dependent interactions by time-resolved luminescence spectroscopy. Environ. Sci. Technol. **50**, 3706 (2016).
37. Carnall, W. T., Fields, P. R., Rajnak, K.: Electronic energy levels of trivalent lanthanide aquo ions. IV. Eu^{3+}. J. Chem. Phys. **49**, 4450 (1968).
38. Dryer, D. J., Korshin, G. V., Fabbricino, M.: In situ examination of the protonation behavior of fulvic acids using differential absorbance spectroscopy. Environ. Sci. Technol. **42**, 6644 (2008).
39. Janot, N., Reiller, P. E., Korshin, G. V., Benedetti, M. F.: Using spectrophotometric titrations to characterize humic acid reactivity at environmental concentrations. Environ. Sci. Technol. **44**, 6782 (2010).

40. Yan, M., Dryer, D., Korshin, G. V.: Spectroscopic characterization of changes of DOM deprotonation–protonation properties in water treatment processes. Chemosphere **148**, 426 (2016).
41. Plancque, G., Moulin, V., Toulhoat, P., Moulin, C.: Europium speciation by time-resolved laser-induced fluorescence. Anal. Chim. Acta **478**, 11 (2003).
42. Vercouter, T.: Complexes aqueux de lanthanides (III) et actinides (III) avec les ions carbonates et sulfates. Etude thermodynamique par spectrofluorimétrie laser résolue en temps et spectrométrie de masse à ionisation électrospray (2005), Université Evry-Val d'Essonne, Evry, France, p. 253.
43. Horrocks, W. D., Jr., Sudnick, D. R.: Lanthanide ion probes of structure in biology. Laser-induced luminescence decay constants provide a direct measure of the number of metal-coordinated water-molecules. J. Am. Chem. Soc. **101**, 334 (1979).
44. Reiller, P. E., Brevet, J., Nebbioso, A., Piccolo, A.: Europium(III) complexed by HPSEC size-fractions of a vertisol humic acid: small differences evidenced by time-resolved luminescence spectroscopy. Spectrochim. Acta, Part A **78**, 1173 (2011).
45. Plancque, G., Maurice, Y., Moulin, V., Toulhoat, P., Moulin, C.: On the use of spectroscopic techniques for interaction studies, Part I: complexation between europium and small organic ligands. Appl. Spectrosc. **59**, 432 (2005).
46. Kuke, S., Marmodée, B., Eidner, S., Schilde, U., Kumke, M. U.: Intramolecular deactivation processes in complexes of salicylic acid or glycolic acid with Eu(III). Spectrochim. Acta, Part A **75**, 1333 (2010).
47. Kimura, T., Choppin, G. R.: Luminescence study on determination of the hydration number of Cm(III). J. Alloys Compd. **213**, 313 (1994).
48. Marmodée, B., Jahn, K., Ariese, F., Gooijer, C., Kumke, M. U.: Direct spectroscopic evidence of 8- and 9-fold coordinated europium(III) species in H_2O and D_2O. J. Phys. Chem. A **114**, 13050 (2010).
49. Pearson, F. J.: Opalinus Clay Experimental Water: A1 Type, Version 980318 (1998), Paul Scherrer Institut, Report Technical Report TM-44-98-07, Villigen, Switzerland.
50. de Craen, M., Wang, L., Van Geet, M., Moors, H.: Geochemistry of Boom Clay Pore Water at the Mol site (2004), SCK•CEN, Report SCK•CEN-BLG-990, Mol, Belgium. p. 181.
51. Gaucher, E. C., Blanc, P., Bardot, F., Braibant, G., Buschaert, S., Crouzet, C., Gautier, A., Girard, J.-P., Jacquot, E., Lassin, A., Negrel, G., Tournassat, C., Vinsot, A., Altmann, S.: Modelling the porewater chemistry of the Callovian-Oxfordian formation at a regional scale. C. R. Geosci. **338**, 917 (2006).
52. Pointeau, I., Coreau, N., Reiller, P. E.: Uptake of anionic radionuclides Cl^-, I^-, SeO_3^{2-} and CO_3^{2-} onto degraded cement pastes and competing effect of organic ligands. Radiochim. Acta **96**, 367 (2008).

Supplemental Material: The online version of this article (DOI: 10.1515/ract-2016-2691) offers supplementary material, available to authorized users.